

Received June 3, 2019, accepted July 19, 2019, date of publication August 27, 2019, date of current version September 12, 2019.

Digital Object Identifier 10.1109/ACCESS.2019.2937792

Robust Indoor Localization in a Reverberant Environment Using Microphone Pairs and Asynchronous Acoustic Beacons

SATOKI OGISO^{1,2}, (Member, IEEE), KOICHI MIZUTANI^{2,3}, NAOTO WAKATSUKI^{2,3},
AND TADASHI EBIHARA^{2,3}, (Member, IEEE)

¹Department of Electronic Control Systems, National Institute of Technology, Gifu College, Motosu 501-0495, Japan

²Graduate School of Systems and Information Engineering, University of Tsukuba, Tsukuba 305-8573, Japan

³Faculty of Engineering, Information and Systems, University of Tsukuba, Tsukuba 305-8573, Japan

Corresponding author: Satoki Ogiso (ogiso@gifu-nct.ac.jp)

This work was supported in part by the Japan Society for the Promotion of Science (JSPS) KAKENHI under Grant JP19K20305, and in part by the OGAWA Science and Technology Foundation.

ABSTRACT In this paper, a robust indoor localization method using microphone pairs and asynchronous acoustic beacons was proposed. The proposed method is applicable even with a two-channel microphone pair, which is the minimal configuration of a microphone array. The proposed method estimates location by using the cross-correlation functions of the measured signals as location likelihoods. Three experiments were conducted to evaluate the proposed method. Four beacons were located at the corners of a localizing area of 4 m by 4 m and emitted signals with a bandwidth of 2 kHz. The localization results were compared to the previous method with deterministic direction-of-arrival estimation. The 90th percentiles of the localization error were 0.23 m for the proposed method with two microphones, 0.19 m for the proposed method with four microphones, and 0.30 m for the previous method under conditions without significant reverberation. Under a condition with reflective walls, the 90th percentile of the localization error of the previous method increased to 0.49 m, while that of the proposed method was only increased to 0.23 m for two microphones and 0.19 m for four microphones. The proposed method contributes to a robust localization in indoor environments and relieves the constraints of receiver configuration.

INDEX TERMS Acoustic beacons, cross correlation, indoor localization, microphone pairs, particle filter.

I. INTRODUCTION

Location estimation is one of the key technologies in the design of a more accessible and convenient infrastructure. The localization problem can be divided into the outdoor and indoor localizations. The outdoor localization problem is usually solved by using a Global Navigation Satellite System (GNSS) such as the Global Positioning System (GPS) or Quasi-Zenith Satellite System (QZSS) [1]. These methods provide up to centimeter-grade accuracy for outdoor localization. On the other hand, achieving centimeter-grade accuracy for indoor localization is a challenging problem. The main difficulty with the indoor localization is the signal fluctuation caused by the structure of the building. The signals from the beacons follow complex paths through the building and sometimes cannot be received due to their non-line-of-sight (NLOS) propagation [2]–[4].

The associate editor coordinating the review of this article and approving it for publication was Lin Wang.

To solve this problem, the indoor localization is usually achieved using two types of methods: beacon-free methods and beacon-based methods. Typical examples of the beacon-free localization are the Light Detection And Ranging (LIDAR)-based or camera-based methods [5], [6]. These localization methods provide high accuracy, but the sensor is still expensive. Also, these methods cannot recognize different rooms with the same shape, and often cannot track locations if the angle of view is occupied by a wall or floor. The beacon-based methods use beacons, which emit known signals from known locations. One of the simplest and most inexpensive version uses Bluetooth Low Energy (BLE) beacons or WiFi routers and measures the amplitude of the radio wave signal [7]. In this approach, the amplitude map is measured in advance [8]. The amplitude map is called a “fingerprint” and the localization is achieved by pattern matching with measured amplitudes and the fingerprint [9]. However, the fingerprint tends to suffer variation due to the interference and the changes in the environment, even

with human movements. As a result of such disturbance, the localization accuracy of the fingerprinting methods has been determined as only about 2 m or higher [7]. Although attempts have been made to resolve these difficulties, sub-meter order accuracy has still not been achieved [10]–[12]. Accurate indoor localization is usually achieved by using the phase or time information rather than the amplitude [13]. For the radio wave, a pulse-like wave called the Ultra Wide Band (UWB) is used to accurately measure the accurate range between the beacon and the receiver [14]–[16]. Although the UWB achieves centimeter-grade accuracy, the hardware for UWB localization consists of specialty transceivers that are not readily available in consumer devices, and thus this method is not widely used.

With this background, the localization method using acoustical signals has attracted attention [17]. The methods use backgrounding with acoustical communications [18], [19], and are applied to the communication with beacons [20]. The phase or time difference is easily measured, because the speed of sound (approx. 3×10^2 m/s) is much slower than the speed of light (approx. 3×10^8 m/s) [21]. To exploit this difference in speed, the acoustic beacon emits encoded sound from beacons located on known locations. The localization methods using time information can be divided into three types: Time-Of-Arrival (TOA)-based methods, Time-Difference-Of-Arrival (TDOA)-based method, and Direction-Of-Arrival (DOA)-based method. TOA-based methods are the most accurate methods among them. The TOA, or Time-Of-Flight (TOF) in some reports, is measured by using time-synchronized beacons and receivers [2], [22]. Then the location of the receiver is estimated by trilateration. While this approach achieves high accuracy, the synchronization of the beacons and receivers requires additional hardware such as radio wave transceivers [23]. Several attempts have been made to measure TOA without time synchronization, such as by using transponders [24]. However, these methods have restrictions e.g, the localization can only be achieved one receiver at a time. The TDOA-based methods were developed to solve the synchronization problem between beacons and receivers [25]–[27]. The TDOA-based methods only measure time differences between the signals of the synchronized beacons at the receivers. The location can then be estimated as the intersection point of the hyperbola lines which correspond to the TDOA and known beacon locations. These methods only require the synchronization of the beacons: the receivers can be synchronization-free. However, the synchronization of all beacons is still a problem if the beacons are in a large facility. For a completely synchronization-free method, the DOA-based approach was proposed [28], [29]. The DOA-based methods measure DOA, sometimes referred as Angle-Of-Arrival (AOA), of the beacon signals with some sensors on a receiver. Then the location is estimated as the intersection point of the lines corresponding to the measured DOA and known beacon locations. The DOA measurement requires the synchronization of the microphones on the receiver, which is easily achieved.

However, the problem of DOA-based acoustic localization is its limited robustness against signal fluctuations and the complexity of the receiver. The DOA estimation is achieved by the cross-correlation functions of the microphone array signals; these functions measure the differences in the time of arrival of the beacon signal between the microphones [29]. The peak time of the cross-correlation corresponds to the DOA. If there are severe reverberations in the environment, the peak time sometimes does not correspond to the DOA [30], [31]. The error of DOA is magnified by the distance from the beacon to the receiver and causes large location error than the TOA or TDOA errors [32]. If a robust localization with DOA is achieved, synchronization-free indoor localization may be very useful, especially in a large environment. Also, the DOA measurement itself requires a relatively complex receiver with multiple microphones. For example, a mobile robot measures DOA with a 32-channel spherical microphone array [33], 32-channel planar microphone array [34], or 4-channel planar microphone array [29]. If the number of the microphone in the array is as low as 2, the DOA has cone-shaped ambiguity and cannot be uniquely determined. The previous methods are not applicable for this situation. If the localization could be accomplished even with a 2-channel microphone pair, which is the minimal configuration of a microphone array, it would be ideal for implementation on smartphones or small objects.

We consider all of the above problems arise from the fact that the multimodal ambiguity of the DOA is not considered in the localization method. The previous methods regard the DOA as a uniquely determined value, and only consider unimodal distributions such as Gaussian distributions around the unique DOA. We propose a method of estimating location using a location likelihood defined by the cross-correlation function of the microphone pairs. The proposed method does not require the deterministic DOA estimation, but rather evaluates location candidates by location likelihood. The proposed method was previously suggested to be robust in a reverberant environment [35], but the location likelihood itself was not discussed and the robustness has not been verified with experimental results such as NLOS or strong reflective waves. In this paper, the proposed method was evaluated using three experiments and the results were discussed with the location likelihood maps for each experiment. The proposed method was applied to 2-channel and 4-channel microphone arrays and compared with a previously proposed method [29]. The computational times for the localization were measured in order to discuss feasibility.

II. PROPOSED METHOD OF ESTIMATING LOCATION

A. DEFINITION OF A LOCATION LIKELIHOOD BY THE CROSS-CORRELATION FUNCTION

The definition of a location likelihood using the cross-correlation function of the microphone pair signals is proposed in this section. This is the core contribution of this study. The location of a localizing target in two-dimensional space is represented as a vector $\mathbf{x}(t) = [x(t), y(t), \theta(t)]^T$,

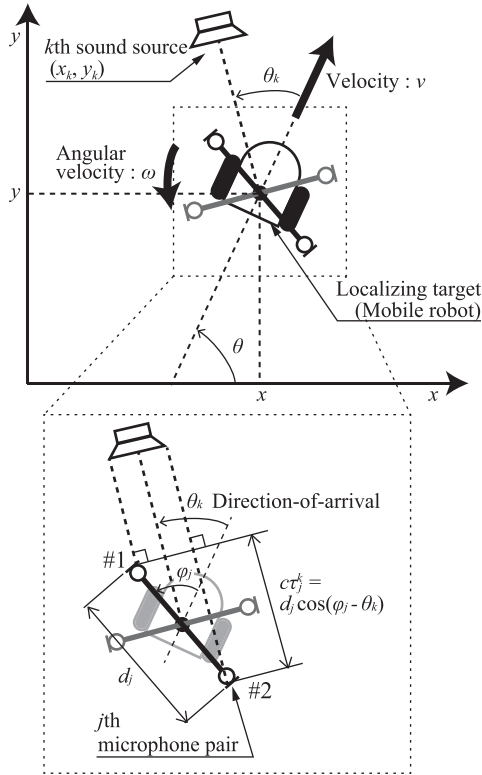


FIGURE 1. Coordinate system used in the proposed method.

where $x(t), y(t)$ are the locations in two-dimensional space, and $\theta(t)$ is the orientation of the localizing target. Figure 1 shows the coordinate system used in the proposed method. The purpose of the localization is to estimate an $x(t)$ which is close to the ground truth. For evaluating and minimizing the difference between an estimated location and the ground truth, a location likelihood metrics is required.

The proposed method uses beacon signals received by microphone pairs on the localizing target. The proposed method assumes that M beacons are deployed in the field with known locations $\mathbf{x}_k = [x_k, y_k]^T (k \in M)$, and N pairs of microphones are placed at the localizing target. If the localizing target is at a location of $\mathbf{x}(t)$, the direction-of-arrival (DOA) of the k th beacon signal $\theta^k(t)$ is uniquely determined by the following equation.

$$\begin{aligned} \theta^k(t) &= \text{atan2}(y(t) - y_k, x(t) - x_k) - \theta_i(t) \\ &\equiv h(\mathbf{x}(t), \mathbf{x}_k), \end{aligned} \quad (1)$$

where $\text{atan2}(y, x)$ returns the angle θ of the location vector (x, y) in the range of $-\pi \leq \theta \leq \pi$. The microphones on the localizing target receive the signal from the DOA of $\theta^k(t)$. Assume that the j th microphone pair is set on the localizing target with an angle of ϕ_j and the d_j is the distance between the microphones. The signal from DOA of $\theta^k(t)$ causes a time difference of $\tau_j^k(t)$ to the microphone pair expressed by the following equation;

$$\tau_j^k(t) = d_j \cos(\theta^k(t) - \phi_j) / c, \quad (2)$$

where c is the speed of sound. Let us denote the recorded signals of the microphone pair by $m_{j,1}^k(t)$ and $m_{j,2}^k(t)$. The cross-correlation function of these microphone signals $R_j^k(\tau)$ is defined by the following equation;

$$R_j^k(\tau) = \int_{T-w}^T m_{j,1}^k(t) m_{j,2}^k(\tau - t) dt. \quad (3)$$

This function takes the maximum value at the time delay of $\tau_j^k(t)$, which corresponds to the DOA $\theta^k(t)$. Conventional localization methods detect the maximum value of $R_j^k(\tau)$ and use the corresponding time delay as a unique DOA measurement. However, detection of the exact DOA from noisy $R_j^k(\tau)$ is difficult under reverberation or other disturbances. Once the misdetection of DOA occurs, it causes huge localization error. This detection of unique DOA makes previous methods vulnerable to the reverberation and other disturbances.

We propose a location likelihood using the above relations as shown in Fig. 2. Assume that we are evaluating the location likelihood of a location candidate $\mathbf{x}_i(t)$. The time delay between the microphone pair is a function of location $\mathbf{x}_i(t)$ and \mathbf{x}_k as shown in the following equation.

$$\tau_j^k(t) = d_j \cos(h(\mathbf{x}_i(t), \mathbf{x}_k) - \phi_j) / c \equiv \bar{\tau}_j^k(\mathbf{x}_i(t)). \quad (4)$$

Each location $\mathbf{x}_i(t)$ corresponds to a unique time delay $\bar{\tau}_j^k(\mathbf{x}_i(t))$ of the cross-correlation function $R_j^k(\tau)$. The likelihood of this time delay $\bar{\tau}_j^k(\mathbf{x}_i(t))$ can be evaluated by looking up the measured cross-correlation function $R_j^k(\tau)$, as $R_j^k(\tau)$ takes a higher value when the sounds of the microphone pair are highly correlated. With this function, the likelihood of the location candidate $\mathbf{x}_i(t)$ with measurement of k th sound source by j th microphone pair is defined as

$$p(R_j^k(\tau)|\mathbf{x}_i(t)) = L_j^k(\mathbf{x}_i(t)) \equiv C(R_j^k(\bar{\tau}_j^k(\mathbf{x}_i(t)))) \quad (5)$$

where the function C is an arbitrary function which maps cross-correlation to the likelihood. The C is assumed to be an envelope detector in this paper. The function in Eq. 5 projects the cross-correlation function, which represents the DOA likelihood, to the localizing state space $\mathbf{x}_i(t)$ as the location likelihood. The location likelihood of the location candidate $\mathbf{x}_i(t)$ with all sound sources and all microphone pairs is then calculated as the product of the likelihoods.

$$p(\mathbf{R}|\mathbf{x}_i(t)) \propto \prod_j^N \prod_k^M p(R_j^k(\tau)|\mathbf{x}_i(t)) = \prod_j^N \prod_k^M L_j^k(\mathbf{x}_i(t)). \quad (6)$$

Here, $\mathbf{R} = [R_1^1, \dots, R_1^M, R_2^1, \dots, R_j^k, \dots, R_N^M]$. The proposed method estimates the location based on the above likelihood. The proposed method achieves localization without detection of single DOA so that it is anticipated to be more robust against the disturbances. The gray-scale image in the Fig. 2 shows an example of the proposed location likelihood $p(\mathbf{R}|\mathbf{x}_i(t))$ for every location in the area.

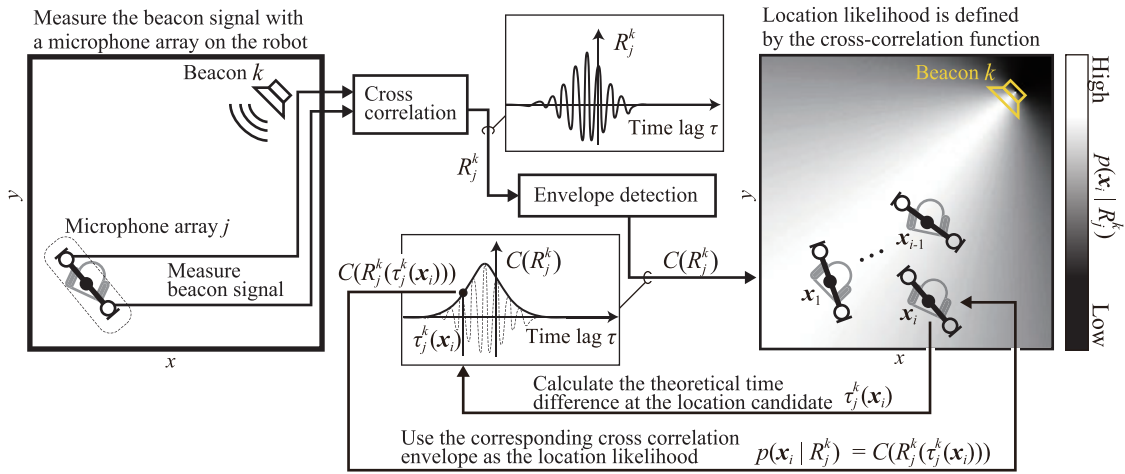


FIGURE 2. Definition of the proposed location likelihood.

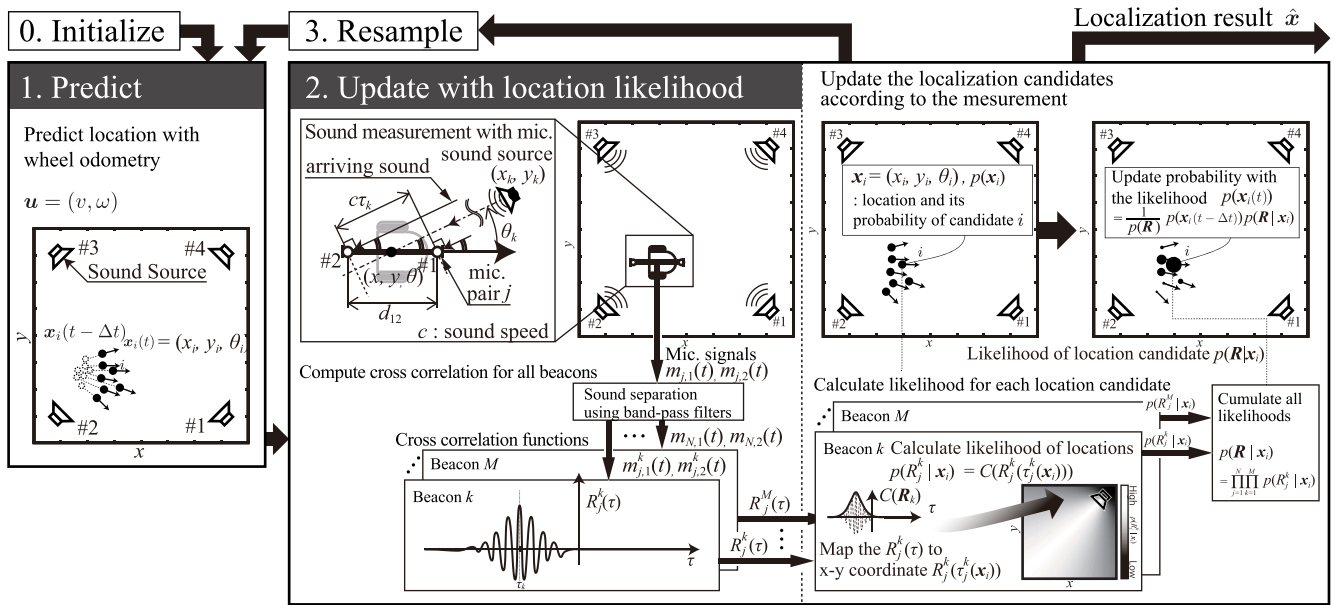


FIGURE 3. Overview of the proposed method using location likelihood.

B. LOCALIZATION BY PARTICLE FILTER WITH THE PROPOSED LOCATION LIKELIHOOD

The proposed method is based on the particle filter algorithm with the cross-correlation functions of microphones as location likelihoods. The particle filter is an algorithm which approximates the probability density function of the location with the Monte-Carlo method. These location candidates are called “particles”. The particle filter can simulate arbitrary likelihood for estimation unlike Kalman filters which assumes the likelihood as Gaussian. It is suitable for the proposed method which uses arbitrary shape of the cross-correlation function as likelihood function. The overview of the proposed method is shown in Fig. 3. The proposed method consists of mainly two parts. Before starting the localization, all locations are initialized. First, the proposed method predicts the location of each particle from the wheel rotation

information of the mobile robot. Second, the location likelihoods of each particle are evaluated with the proposed location likelihood with cross-correlation function. The microphone signals are used in this step. Then the particles are resampled to balance the weights of the particles.

In the first step, the wheel rotation information provides the velocity and angular velocity of the mobile robot. Let us denote the velocity as v and the observed angular velocity as ω . The i th location candidate $x_i(t)$ at the time t is predicted as

$$\begin{aligned}
 x_i(t) &= f(x_i(t - \Delta t), v, \omega) \\
 &= \begin{bmatrix} x_i(t - \Delta t) \\ y_i(t - \Delta t) \\ \theta(t - \Delta t) \end{bmatrix} + \begin{bmatrix} v \cos(\theta(t - \Delta t)) \\ v \sin(\theta(t - \Delta t)) \\ \omega \end{bmatrix} \Delta t, \quad (7)
 \end{aligned}$$

TABLE 1. Condition of experiments.

Sampling frequency of microphones	100	kHz
Sound characteristics		
Sound type	Linear up chirp	
Sweeping time	0.1	s
Sweeping frequencies		
Sound 1	12 – 14	(kHz)
Sound 2	14.5 – 16.5	(kHz)
Sound 3	17 – 19	(kHz)
Sound 4	19.5 – 21.5	(kHz)

where Δt denotes the time step of the estimation. In realistic situations, the velocity and angular velocity contain measurement noises. In this paper, these values are assumed to be samples from Gaussian distributions $n_v \sim \mathcal{N}(v, \sigma_v^2)$ and $n_\omega \sim \mathcal{N}(\omega, \sigma_\omega^2)$, where σ_v^2 and σ_ω^2 are the variations caused by sensor noises. The Monte-Carlo method is performed to sample from these probability density functions. Locations of each location candidate are predicted by Eq. 7 with a sample of velocity and angular velocity from above Gaussian.

The second step consists of updating the particles by the location likelihood. The microphone signals are measured in this step and the cross-correlation functions $\mathbf{R} = [R_1^1, \dots, R_1^M, R_2^1, \dots, R_j^k, \dots, R_N^M]$ are calculated for all microphone pairs and all sound sources. Then, the location likelihood is calculated for each location candidate $\mathbf{x}_i(t)$ by Eq. 6. Each location candidate has corresponding probability $p(\mathbf{x}_i(t))$, which represents the probability that the candidate $\mathbf{x}_i(t)$ is the true location. This probability is updated by measurement \mathbf{R} with the following Bayes' theorem.

$$\begin{aligned}
 p(\mathbf{x}_i(t)|\mathbf{R}) &= \frac{1}{p(\mathbf{R})} p(\mathbf{x}_i(t - \Delta t)) p(\mathbf{R}|\mathbf{x}_i(t)) \\
 &= \frac{1}{p(\mathbf{R})} p(\mathbf{x}_i(t - \Delta t)) \prod_j^N \prod_k^M L_j^k(\mathbf{x}_i(t)), \quad (8)
 \end{aligned}$$

where $p(\mathbf{R})$ represents the normalizing factor of the probability. The localization result $\mathbf{x}(t)$ is calculated as the expected value of the probability $p(\mathbf{x}_i(t)|\mathbf{R})$,

$$\hat{\mathbf{x}}(t) = \sum_i p(\mathbf{x}_i(t)|\mathbf{R}) \mathbf{x}_i(t). \quad (9)$$

The localization is achieved by doing the above steps recursively by replacing $p(\mathbf{x}_i(t - \Delta t))$ with the new probability $p(\mathbf{x}_i(t)|\mathbf{R})$. The particles are resampled if the number of the effective particles is below a threshold. The number of the effective particles is calculated by following equation.

$$N_{\text{effec}} = N(\sum_{i=1}^N p(\mathbf{x}_i(t)|\mathbf{R})^2)^{-1}. \quad (10)$$

The pseudo-code of the proposed method is shown in Algorithm 1.

III. EXPERIMENTAL CONDITIONS

The proposed method was evaluated by a localization experiment in a room. Figure 4(a) shows the experimental setup of the localizing target. The localizing target consists of two

Algorithm 1 Localization With the Proposed Likelihood

```

1: Define a vector array of location candidates  $\mathbf{x}$ 
2: Define an array of corresponding location probabilities  $\mathbf{p}$ 
3: Define and initialize localization result  $\hat{\mathbf{x}}$ 
4:
5: for each particle  $i$  do
6:   Initialize vector of location  $\mathbf{x}_i$ 
7:   Initialize corresponding location probability  $p_i$ 
8: end for
9:
10: repeat
11:    $\mathbf{m} \leftarrow$  data from microphone pairs
12:   for each sound source  $k$  do
13:      $\mathbf{m}^k \leftarrow$  SeparateSoundSources( $\mathbf{m}, k$ )
14:     for each microphone pair  $j$  do
15:        $\mathbf{R}_j^k \leftarrow$  Correlation( $m_{j,1}^k, m_{j,2}^k$ ) (Eq. 3)
16:     end for
17:   end for
18:
19:    $\mathbf{u} \leftarrow$  data from wheel rotation
20:   for each particle  $i$  do
21:      $\mathbf{x}_{pred,i} \leftarrow$  PredictLocation( $\mathbf{x}_i, \mathbf{u}$ ) (Eq. 7)
22:      $l_{pred,i} \leftarrow p_i \cdot \text{Likelihood}(\mathbf{x}_{pred,i}, \mathbf{R})$  (Eq. 8)
23:   end for
24:   for each particle  $i$  do
25:      $p_i \leftarrow l_{pred,i} / \sum_i l_{pred,i}$ 
26:   end for
27:    $\hat{\mathbf{x}} \leftarrow \sum_i p_i \mathbf{x}_{pred,i}$  (Eq. 9)
28:
29:   if  $N_{\text{effec}}$  (Eq. (10)) < threshold then
30:      $\mathbf{x} \leftarrow$  Resample( $\mathbf{x}_{pred}, \mathbf{p}$ )
31:   else
32:      $\mathbf{x} \leftarrow \mathbf{x}_{pred}$ 
33:   end if
34: until localization ends

```

microphone pairs and a mobile robot platform. The distances of the microphones were $d_1 = d_2 = 0.25$ m. The angles of the microphone pairs were $\phi_1 = 0$ rad and $\phi_2 = \pi/2$ rad. MEMS microphones (SPU0414HR5H-SB; Knowles) were used face upward as omnidirectional microphones in the horizontal plane. The microphone signals were recorded with an AD converter (NI USB-6212; National Instruments) at a sampling frequency of 100 kHz. The wheel rotation of the mobile robot was measured at a frequency of 5 Hz. The proposed method estimated the location every time when the wheel rotation was measured. In every estimation step, the cross-correlation functions were calculated with the most recent microphone signals with a window length of $w = 0.1$ s.

The experiments were carried out under three sets of conditions. The common condition for these experiments is shown in Fig. 4(b). The mobile robot is assumed to be in a room with four beacons at the corners. The mobile robot runs a path shown in the figure. The path was designed

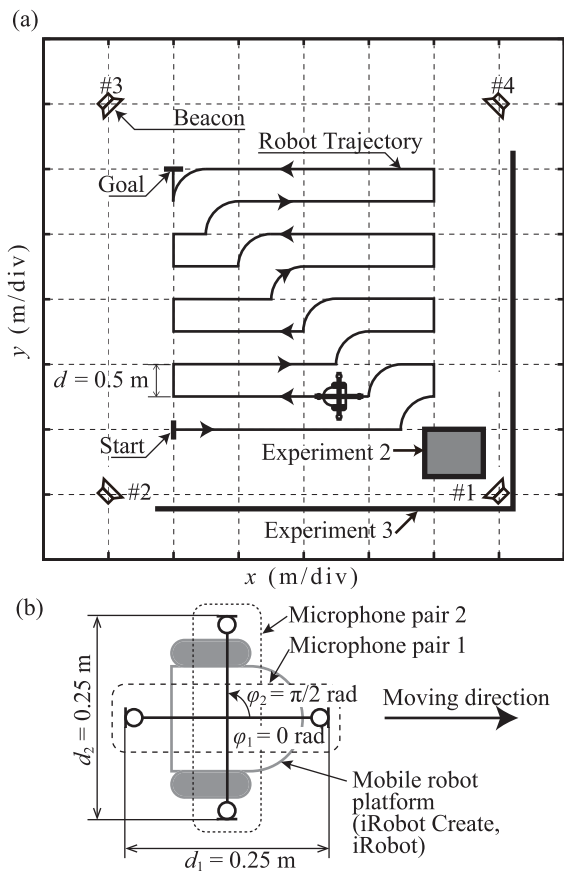


FIGURE 4. Experimental setup for evaluating localization methods. (a) Beacon setup and evaluated path. (b) Localizing target and microphone pair configuration.

to include straight lined, curved lined and turning in the area. The mobile robot runs on the straight line at a speed of 0.25 m/s. The four beacons emit up-chirp signals at the different frequency ranges shown in Table 1. The beacons emit signals continuously without interval. The received signals at the microphones were separated by band-pass filters with corresponding pass bands for each beacon. The band-pass filters were implemented as 100-tap finite impulse response filters. While the tap number is decreased from the previous research to reduce calculation cost [29], it is enough for separating the beacons. The bands of the filters were set at $(0.99f_{\text{start}}, 1.01f_{\text{stop}})$ for each beacon with frequency bands of $f_{\text{start}}-f_{\text{stop}}$ (Hz). The cross-correlation function was calculated for each microphone pair shown in Fig. 4. Experiment 1 was carried out without any obstacle or any reflective walls close to the beacon. The robot traveled the path 10 times in experiment 1. A cardboard box was placed in front of the Beacon #1 in experiment 2 in order to evaluate the robustness of the localization against NLOS. The robot traveled the path for 10 times in the experiment 2. In experiment 3, reflective walls were placed behind beacon #1 as shown in Fig. 4 in order to evaluate the robustness of the localization against strong reflective waves. The robot traveled the path 8 times

in experiment 3. For each condition, the proposed method was applied to estimate the location of the mobile robot. The proposed method estimated the location using two pairs of microphones (4 microphones in total), or one pair of microphones (2 microphones in total). The parameters of the proposed method were set by a preliminary experiment. The variations of the wheel rotation were set as $\sigma_v = 0.3$ m/s and $\sigma_\omega = 0.1$ rad/s. The number of location candidates were set as 1000. The proposed method was compared to a previously proposed localization method using DOA and an extended Kalman filter [29]. This previous method uses four microphones to estimate a unique DOA. The true location was measured with an optical tracking system. The system consists of 18 cameras (OptiTrack Prime 41; OptiTrack) and analysis software (Motive Body; OptiTrack). The frame rate of the true location was 120 Hz. The estimation result at 5 Hz was compared with the true location sampled at the closest time.

The number of particles in the proposed method affects the localization accuracy and computational cost. To examine the effect of the number of particles, the computational time and localization accuracy for different numbers of particles were examined. The localization evaluation and computational time measurement were performed on a personal computer (CPU: Intel Core i5-4670 (3.4 GHz); memory: 16 GB; Operating System: Microsoft Windows 10).

For quantitatively examine the reverberation and reflection of the environment, impulse responses and reverberation time 60 (RT60) were measured. The measurement was performed with a microphone (Type 4939-A-011; B&K) and an amplifier (Type 2690-0S2; B&K) located at the start point in Fig. 4. A loudspeaker was located at the location of the sound source #1. A log-swept-sine signal with a sweep time of 5 second from 0 Hz to 50 kHz was used for the measurement of the impulse response. The signal was generated from an AD/DA converter (NI USB-6221 BNC; National Instruments) at a sampling frequency of 100 kHz. Then the signal was supplied to the loudspeaker through a first-order low pass filter with a cutoff frequency of 50 kHz and an audio amplifier (AP05; Fostex). The signal was measured with the microphone and the AD/DA converter at a sampling frequency of 100 kHz. The measured signal was processed on a personal computer to obtain impulse response. For a better signal-to-noise ratio, the measurement was performed for 100 times and the measured signals were synchronously added. The energy decay curve was measured as a Schroeder's integration of the measured impulse response. The RT60 was measured as 3 times -20 dB decay time from -10 dB to -30 dB of the energy decay curve. The above procedure was performed with and without the reflective walls shown in Fig. 4.

The measured energy decay curves and impulse responses with and without the walls are shown in Fig. 5. The RT60 without the wall was 1.62 s and that with the wall was 1.51 s. While these two were slightly different, the reverberation can be regarded almost equal for both conditions.

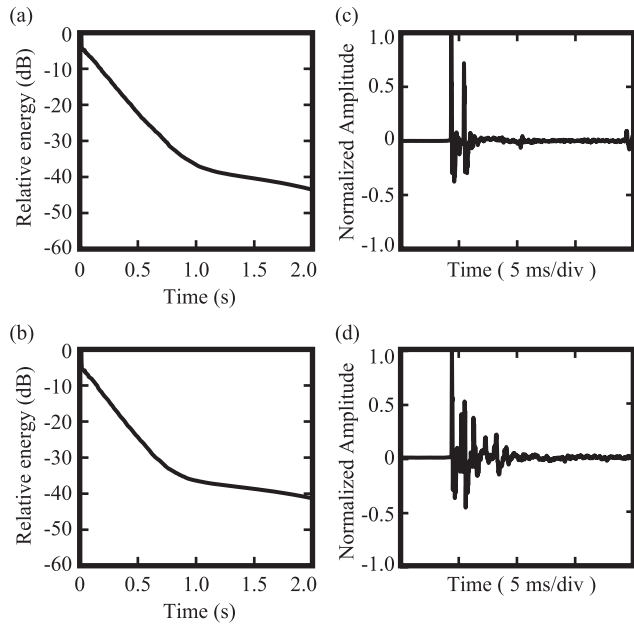


FIGURE 5. Experimental condition of reverberation and reflection. (a) Energy decay curve without the wall, (b) energy decay curve with the wall, (c) close-up of the impulse response without the wall, (d) close-up of the impulse response with the wall.

On the other hand, the reflective waves were different as confirmed in Fig. 5(c)(d). The impulse response without the wall in Fig. 5(c) showed two significant peaks. These peaks correspond to the direct wave and a reflective wave from the nearest wall of the building. On the other hand, The impulse response with the wall in Fig. 5(d) showed more significant peaks than that without the wall. These peaks were made with the wall and may cause problem with direction-of-arrival estimation.

IV. RESULTS AND DISCUSSION

A. EXPERIMENT 1: WITHOUT AN NLOS BEACON OR STRONG REFLECTIVE WAVES

An example of the localization result is shown in Fig. 6, and the localization results for each method are shown in Fig. 7. In Fig. 6(a), it is confirmed that all methods estimate the location without diverging. The boxplot in Fig. 7(a) shows that all methods estimate the location approximately within the accuracy of 1 m. The localization error is relatively large for the previous method with deterministic DOA estimation. The outliers of the error are especially large for the previous method. The 90th percentile errors shown in Fig. 7(b) were 0.21 m for the proposed method with two microphones, 0.19 m for the proposed method with four microphones, and 0.23 m for the previous method. As shown in the Fig. 6(a), the previous method sometimes jumps from the location. The cause of this error is misdetection of the DOA and localization with an incorrect assumption of the location. On the other hand, the proposed method does not have such outliers and the localization result is smoother than in the previous method. This reduction of outliers is possible using the features of the proposed method. The proposed method does not assume deterministic DOA, and it is possible to estimate the true location even if the peak of the cross-correlation function does not correspond to the true DOA. Comparing the two results from the proposed methods, the results with four microphones achieve lower localization error. It is considered that the location likelihood is less ambiguous when four microphones are used, as extra information is obtained. Note that the previously proposed methods cannot estimate the location using only two microphones. Although the proposed method with two microphones has larger error than that with four microphones, it still has less error than

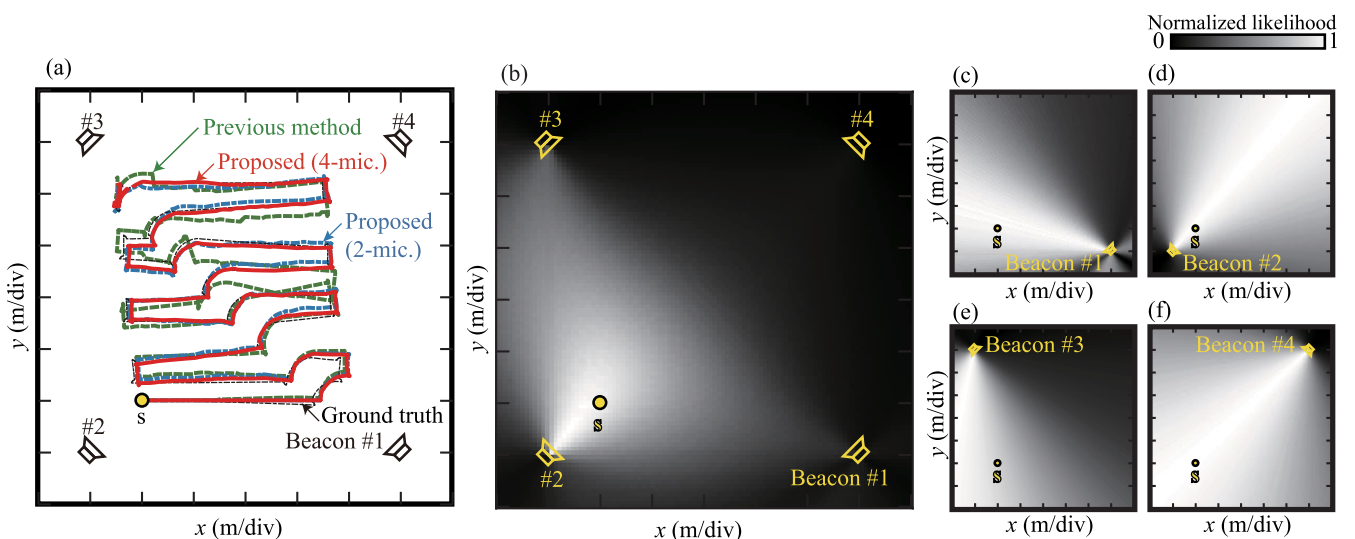


FIGURE 6. An example of the localization result of each method in experiment 1. (a) Localization results for each method. (b) An example of the location likelihood $p(x_i(t)|R)$ at the point s . Panel (c) shows the location likelihood at the point s only with the beacon #1 $p(x_i(t)|R_1^1)p(x_i(t)|R_2^1)$, (d) shows that with the beacon #2 $p(x_i(t)|R_1^2)p(x_i(t)|R_2^2)$, (e) shows that with the beacon #3 $p(x_i(t)|R_1^3)p(x_i(t)|R_2^3)$, and (f) shows that with the beacon #4 $p(x_i(t)|R_1^4)p(x_i(t)|R_2^4)$.

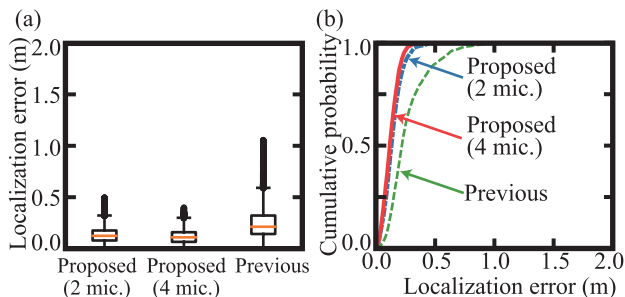


FIGURE 7. Localization error of experiment 1. (a) Box plot of the localization error. (b) Cumulative distribution functions of the localization error.

the previous method with deterministic DOA detection. The location likelihood map calculated from the signals recorded at the start point s is shown in Figs. 6(c)-(f). The limitation of the proposed method is determined by the bandwidth of the beacon signal. The envelope of the cross-correlation function of a chirp signal with bandwidth of f_b Hz has a main lobe with a width of $1/f_b$ Hz [36]. In this study, the bandwidths were 2 kHz for each beacon. The corresponding width of the main lobe of the cross-correlation function is 0.5 ms. On the other hand, the maximum time lag of microphone pair signals was $d_j/c = 0.76$ ms and this time lag corresponds to ± 90 deg of DOA. Although the ratio is not linear, the expected width of the location likelihood is approximately $0.5 \text{ ms}/0.76 \text{ ms} = 66\%$ of the maximum time lag. This expected width corresponds to approximately ± 59 deg of the location likelihood. The likelihood maps in Figs. 6(c)-(f) have approximately this width and are reasonable when compared to the expected width of the high likelihood location. The wider spread of the location likelihood from the theoretical angle can be understood as effects of a reflective wave and reverberation

in the room as shown in Fig. 5. Although further experiments are expected on this topic to improve the accuracy, we focus on the robustness of the proposed method in this paper.

B. EXPERIMENT 2: WITH AN NLOS BEACON

A representative localization result is shown in Fig. 8, and the localization results for each method are shown in Fig. 9. The localization errors of each method were slightly increased from experiment 1 by the no-line-of-sight condition caused by the cardboard box. In Fig. 9(a), the localization error of the outliers of the previous method were increased from approximately 1.1 m to 1.4 m. The proposed methods also increased the localization error, but the error showed resilience, since it was still below the error in the previous method. The 90th percentile errors shown in Fig. 9(b) were 0.23 m for the proposed method with two microphones, 0.19 m for the proposed method with four microphones, and 0.31 m for the previous method. From these results, both methods achieve localization without catastrophic error. Under the NLOS condition, it is not possible to correctly estimate the DOA by means of a deterministic approach. The previous method calculates inconsistencies of the two microphone pairs and reflects them to the localization by adjusting the location feedback constants [29]. The proposed method achieves this robust localization without any special calculations or fine-tuning of the method. In particular, the previously proposed NLOS mitigation technique is not applicable for two microphones. The estimation results were considered robust because the DOA was not measured deterministically, which allowed the estimator to examine possible locations. An example of the localization results is shown in Fig. 8(a). The estimated path of the previous method

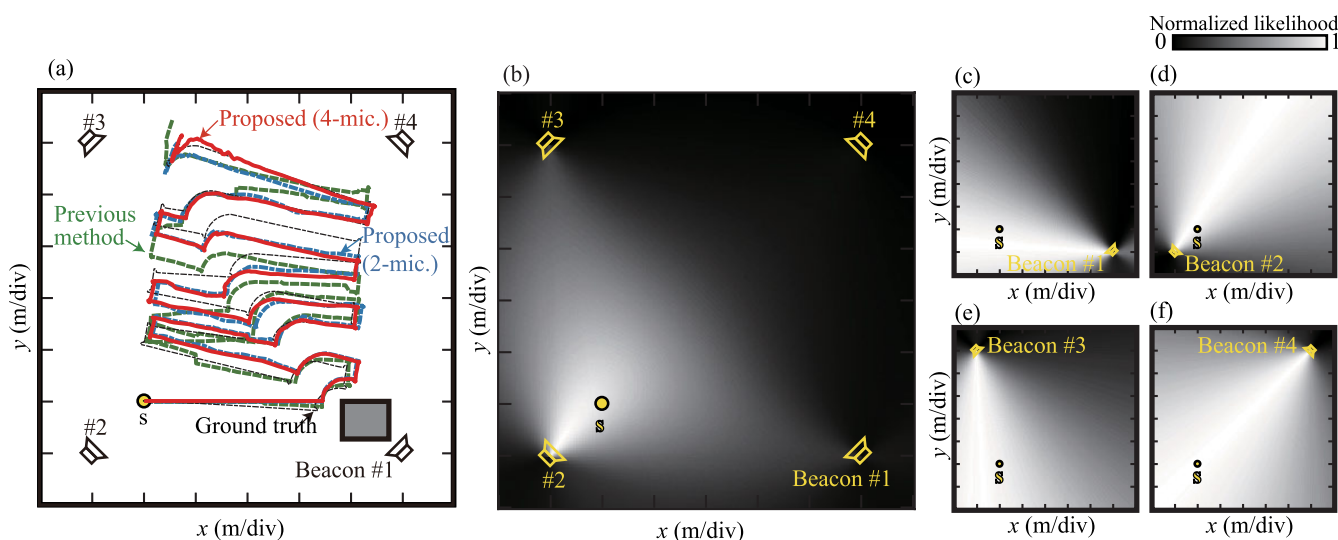


FIGURE 8. An example of the localization result for each method in experiment 2, in which a beacon is NLOS. (a) Localization results of each method. (b) An example of the location likelihood $p(x_i(t)|R)$ at the point s . Panel (c) shows the location likelihood at the point s only with the beacon #1 $p(x_i(t)|R_1^1)p(x_i(t)|R_2^1)$, (d) shows that with the beacon #2 $p(x_i(t)|R_1^2)p(x_i(t)|R_2^2)$, (e) shows that with the beacon #3 $p(x_i(t)|R_1^3)p(x_i(t)|R_2^3)$, and (f) shows that with the beacon #4 $p(x_i(t)|R_1^4)p(x_i(t)|R_2^4)$.

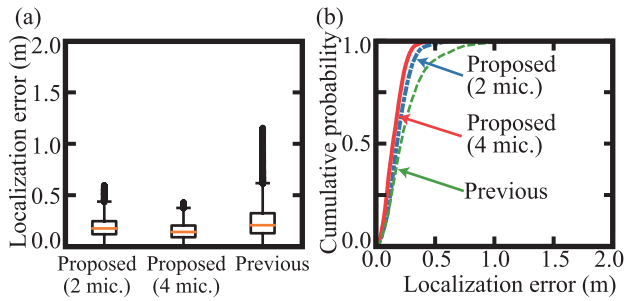


FIGURE 9. Localization error of experiment 2. (a) Box plot of the localization error. (b) Cumulative distribution functions of the localization error.

has some jumps in the localization similar to experiment 1. Also, the location likelihood map calculated from the signals recorded at the start point s is shown in Figs. 8(b)-(f). The proposed method also has slight location error in the middle of the path.

C. EXPERIMENT 3: WITH STRONG REFLECTIVE WAVES

The experimental results are shown in Fig. 11. The reflective walls were placed behind beacon #1 under this condition. The results in Fig. 11(a) confirm that there was a drastic increase of the localization error is confirmed compared to Fig. 7(a). This was caused by the significant reflective waves generated by the reflective walls. In particular, the outliers of the localization error of the previous method increased from 1.1 m to approximately 2 m. Also, the 90th percentile error of the previous method increased from 0.31 m to 0.49 m. As for the proposed method, although the maximum value of outliers increased from 0.7 m to 1.3 m for two microphones and 0.5 m to 1.2 m for four microphones, the 90th percentile error only changed from 0.21 m to 0.23 m for two microphones and

from 0.19 m to 0.23 m for four microphones. Figure 10(a) shows a representative localization result. While the previous method diverged from the true path, the proposed method was relatively unaffected. The location likelihood map calculated from the signals recorded at the start point s is shown in Figs. 10(b). Compared to those in the two experiments above, the likelihood map shows a wide distribution of high likelihood. The cause of this spread is the reflective waves from the reflective walls behind beacon #1. The reflective walls caused strong reflective waves and the waves were recorded at the microphones as the correlated sounds from different directions. As the reflective waves have high correlations with the direct wave, the cross-correlation function becomes a mixture of these signals and the peak spreads. The previous approach does not consider this effect and is not resilient against the multimodal correlation function caused by the reflective waves. The proposed method uses the entire cross-correlation function as location likelihood. As shown in Fig. 10(c), the superposed likelihood of all sounds shows the true location with a larger spread than in Fig. 6(c). The location likelihoods of the inconsistent areas were decreased, which rendered the proposed method robust against reverberation.

D. RELATION OF LOCALIZATION ERROR AND COMPUTATIONAL COST

The localization result of the proposed method is affected by the number of particles. The localization accuracy and robustness may increase if a large number of particles were used. Instead, we found that a large number of particles required a long computational time. Figures 12(a)-(c) and Figs. 13(a)-(c) show the relationship between the number of particles and the localization error for each experiment. All the results show a trend in which the localization error

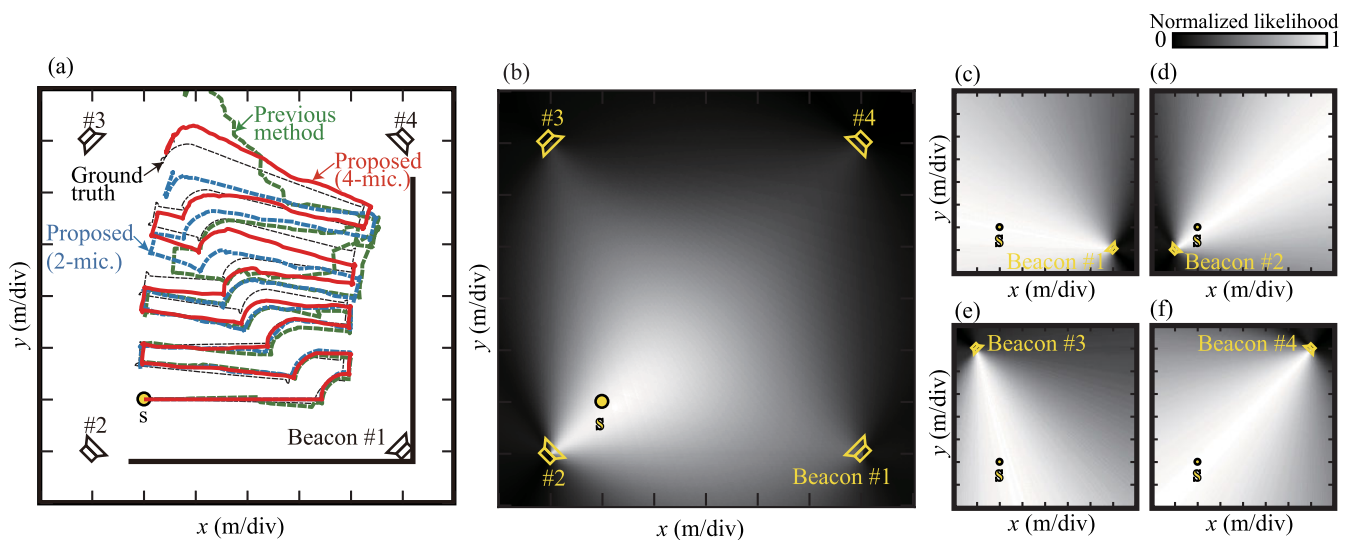


FIGURE 10. An example of the localization result of each method in experiment 3, in which a reflective wall was places just behind the beacons. (a) Localization results of each method. (b) An example of the location likelihood $p(x_i(t)|R)$ at the point s . Panel (c) shows the location likelihood at the point s only with the beacon #1 $p(x_i(t)|R_1^1)p(x_i(t)|R_2^1)$, (d) shows that with the beacon #2 $p(x_i(t)|R_1^2)p(x_i(t)|R_2^2)$, (e) shows that with the beacon #3 $p(x_i(t)|R_1^3)p(x_i(t)|R_2^3)$, (f) shows that with the beacon #4 $p(x_i(t)|R_1^4)p(x_i(t)|R_2^4)$.

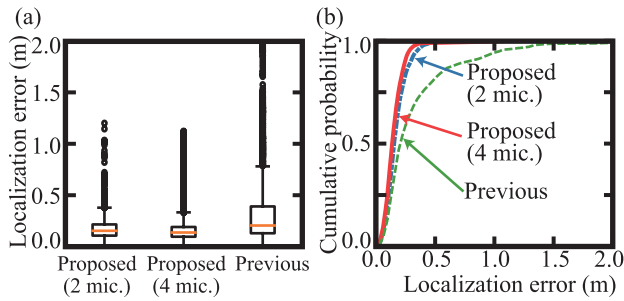


FIGURE 11. Localization error of experiment 3. (a) Box plot of the localization error. (b) Cumulative distribution functions of the localization error.

decreases as the number of particles increases. The number of particles represents a resolution of the likelihood map approximation. If the number of particles is low, the particles may not exist around the location with maximum likelihood. For this example, the localization errors converged if the number of particles was larger than approximately 100. Although the likelihood map depends on the layout of beacons and microphone pairs, the robustness of the proposed method can be discussed with the converged results in this experiment. The converged localization errors may indicate the limitation of the proposed method. Because we used 1000 particles in the previous sections, the results were valid in term of convergence of the localization error. Figure 12(d) and Fig. 13(d) show the relationship between the number of particles and

the computational time. The computational time increases as the number of particles increases. The lower bound of the computational time is approximately 0.05 s with two microphones and 0.08 s with four microphones in this case. Apart from the specifications of the computer, the lower bound of the computational time may be affected by the calculation of cross-correlation functions for each microphone pair. The localization with two microphones requires the cross-correlation function of one pair of microphone, which leads to lower computational time compared to the four microphones. The outliers of the computational time are considered the effect of background processes of the computer. The computational cost of the particle filter algorithm is proportional to the number of particles. If we expect the proposed method to work in real time, the localization should be completed within the sampling frequency of the location. As the sampling frequency of the location is 5 Hz in this case, the proposed method can be used with at least 1000 particles in real time. Also, compared to the computational time of the previous method, the time by the proposed method is the same or lower than the previous method. This is especially true when two microphones were used. In that case, the proposed method requires the computation of cross-correlation function for the single pair of the microphones, which leads to lower computational time without compromising the localization error. Since the localization error converges at this number of particles, the results show the feasibility of the proposed method.

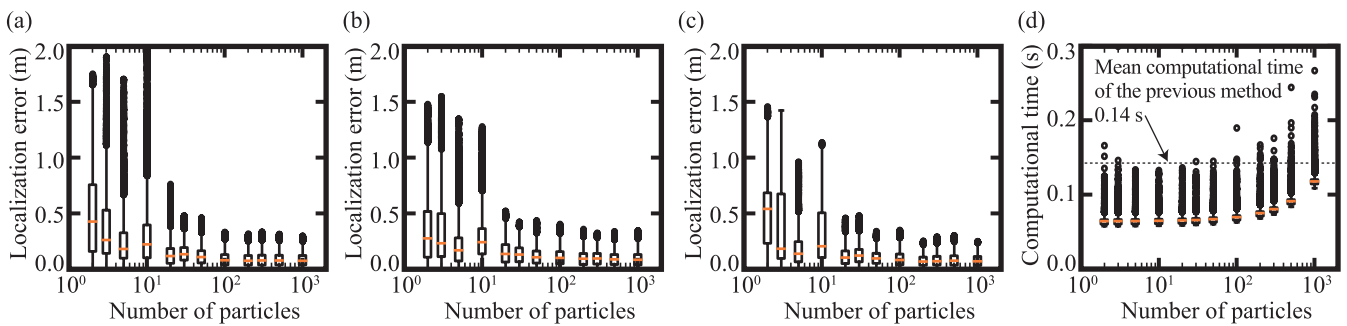


FIGURE 12. Calculation time and localization error for different numbers of particles with two microphones. (a) Relationship between calculation time and number of particles. Panels (b), (c) and (d) depict the relationship between the localization error and number of particles in experiment 1, 2 and 3, respectively.

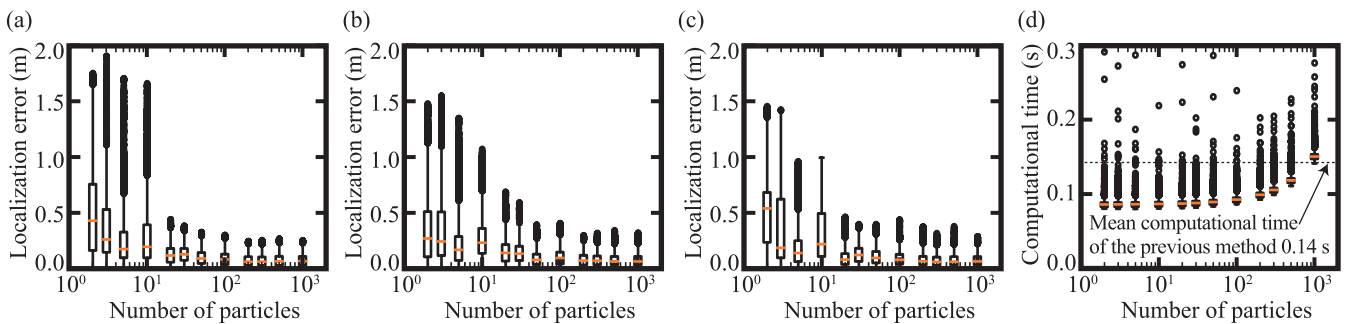


FIGURE 13. Calculation time and localization error for different numbers of particles with four microphones. (a) Relationship between calculation time and number of particles. Panels (b), (c) and (d) depict the relationship between the localization error and number of particles in experiment 1, 2 and 3, respectively.

V. CONCLUSION

An indoor localization method with microphone pairs and asynchronous acoustic beacons was proposed and evaluated with experiments. The proposed method is based on the location likelihood defined by the cross-correlation functions of the microphone array pairs. There are two main contributions of the proposed method: the proposed method achieves robust localization than deterministic DOA measurement; the proposed method is applicable even with a two-channel microphone pair, which is the minimal configuration of a microphone array. The localization was implemented as a particle filter algorithm. The proposed method was evaluated with three experiments, which examined the localization error without disturbance, the localization error with the disturbance of non-line-of-sight and the localization error with the disturbance of reflective walls. Four beacons were located at the corner of a square area and emitted signals with a bandwidth of 2 kHz continuously. A mobile robot with two microphone pairs traveled in the area and its location was estimated with the proposed method and a previous method with deterministic DOA estimation. The result without disturbances showed that the proposed method achieves the 90th percentile of the localization error of 0.19 m and the previous method achieves that of 0.39 m. Under the non-line-of-sight condition, the 90th percentiles of the localization errors were not changed, while the outliers were increased. With the reflective walls, the previous method was greatly affected and the 90th percentile of the localization error was 0.49 m. This condition did not affect the proposed method as much as it did the previous method, and the proposed method achieved a 90th percentile localization error of 0.23 m. The reason for the localization error degradation was the spread of the cross-correlation function, which was fatal for the previous method with a deterministic approach. These results thus showed that the proposed method achieves robust localization by using the location likelihood. Also, the localization error of the proposed method was lower than that of the method using DOA detection even with a pair of microphones. Further studies on localization accuracy and the bandwidth of the beacons are warranted.

REFERENCES

- [1] H. S. Maghdid, I. A. Lami, K. Z. Ghafour, and J. Lloret, "Seamless outdoors-indoors localization solutions on smartphones: Implementation and challenges," *ACM Comput. Surv.*, vol. 48, no. 4, 2016, Art. no. 53.
- [2] I. Güvenç and C.-C. Chong, "A survey on TOA based wireless localization and NLOS mitigation techniques," *IEEE Commun. Surveys Tuts.*, vol. 11, no. 3, pp. 107–124, 3rd Quart., 2009.
- [3] F. Dwiyyasa and M.-H. Lim, "A survey of problems and approaches in wireless-based indoor positioning," in *Proc. 7th Int. Conf. Indoor Positioning Indoor Navigat. (IPIN)*, Oct. 2016, pp. 1–7.
- [4] A. Yassin, Y. Nasser, M. Awad, A. Al-Dubai, R. Liu, C. Yuen, R. Raulefs, and E. Aboutanos, "Recent advances in indoor localization: A survey on theoretical approaches and applications," *IEEE Commun. Surveys Tuts.*, vol. 19, no. 2, pp. 1327–1346, 2nd Quart., 2016.
- [5] S. Thrun, W. Burgard, D. Fox, and R. C. Arkin, *Probabilistic Robotics*. Cambridge, MA, USA: MIT Press, 2006.
- [6] T. Taketomi, H. Uchiyama, and S. Ikeda, "Visual SLAM algorithms: A survey from 2010 to 2016," *IPSI Trans. Comput. Vis. Appl.*, vol. 9, 2017, Art. no. 16.
- [7] M. Murata, D. Ahmetovic, D. Sato, H. Takagi, K. M. Kitani, and C. Asakawa, "Smartphone-based indoor localization for blind navigation across building complexes," in *Proc. IEEE Int. Conf. Pervasive Comput. Commun. (PerCom)*, Mar. 2018, pp. 1–10.
- [8] P. Bahl and V. N. Padmanabhan, "RADAR: An in-building RF-based user location and tracking system," in *Proc. 19th Annu. Joint Conf. Comput. Commun. Societies INFOCOM Conf. Comput. Commun.*, Mar. 2000, pp. 775–784.
- [9] S. He and S.-H. G. Chan, "Wi-Fi fingerprint-based indoor positioning: Recent advances and comparisons," *IEEE Commun. Surveys Tuts.*, vol. 18, no. 1, pp. 466–490, 1st Quart., 2015.
- [10] C. Cai, X. Ma, M. Hu, Y. Yang, Z. Li, and J. Liu, "SAP: A novel stationary peers assisted indoor positioning system," *IEEE Access*, vol. 6, pp. 76475–76489, 2018.
- [11] W. Shao, H. Luo, F. Zhao, Y. Ma, Z. Zhao, and A. Crivello, "Indoor positioning based on fingerprint-image and deep learning," *IEEE Access*, vol. 6, pp. 74699–74712, 2018.
- [12] B. Jang and H. Kim, "Indoor positioning technologies without offline fingerprinting map: A survey," *IEEE Commun. Surveys Tuts.*, vol. 21, no. 1, pp. 508–525, 1st Quart., 2019.
- [13] C. L. Bennett and G. F. Ross, "Time-domain electromagnetics and its applications," *Proc. IEEE*, vol. 66, no. 3, pp. 299–318, Mar. 1978.
- [14] Y. Xu, G. Tian, and X. Chen, "Enhancing INS/UWB integrated position estimation using federated EFIR filtering," *IEEE Access*, vol. 6, pp. 64461–64469, 2018.
- [15] Y. Xu, Y. S. Shmaliy, Y. Li, and X. Chen, "UWB-based indoor human localization with time-delayed data using EFIR filtering," *IEEE Access*, vol. 5, pp. 16676–16683, 2017.
- [16] C. Briso, C. Calvo, and Y. Xu, "UWB propagation measurements and modelling in large indoor environments," *IEEE Access*, vol. 7, pp. 41913–41920, 2019.
- [17] J. Ureña, Á. Hernández, J. J. García, J. M. Villadangos, M. C. Pérez, D. Gualda, F. J. Álvarez, and T. Aguilera, "Acoustic local positioning with encoded emission beacons," *Proc. IEEE*, vol. 106, no. 6, pp. 1042–1062, Jun. 2018.
- [18] T. Ebihara and G. Leus, "Doppler-resilient orthogonal signal-division multiplexing for underwater acoustic communication," *IEEE J. Ocean. Eng.*, vol. 41, no. 2, pp. 408–427, Apr. 2016.
- [19] T. Ebihara, G. Leus, and H. Ogasawara, "Underwater acoustic communication using Doppler-resilient orthogonal signal division multiplexing in a harbor environment," *Phys. Commun.*, vol. 27, pp. 24–35, Apr. 2018.
- [20] K. Mizutani, T. Ebihara, N. Wakatsuki, and K. Mizutani, "Locality of area coverage on digital acoustic communication in air using differential phase shift keying," *Jpn. J. Appl. Phys.*, vol. 48, no. 7s, 2009, Art. no. 07GB07.
- [21] K. Mizutani, N. Wakatsuki, and T. Ebihara, "Introduction of measurement techniques in ultrasonic electronics: Basic principles and recent trends," *Jpn. J. Appl. Phys.*, vol. 55, no. 7S1, 2016, Art. no. 07KA02.
- [22] W. Li, Y. Jia, and J. Du, "TOA-based cooperative localization for mobile stations with NLOS mitigation," *J. Franklin Inst.*, vol. 353, no. 6, pp. 1297–1312, Apr. 2016.
- [23] P. Lazik, N. Rajagopal, O. Shih, B. Sinopoli, and A. Rowe, "ALPS: A Bluetooth and ultrasound platform for mapping and localization," in *Proc. ACM SenSys*, 2015, pp. 73–84.
- [24] H. Iwaya, K. Mizutani, T. Ebihara, and N. Wakatsuki, "Acoustical positioning method using transponders with adaptive signal level normalizer," *Jpn. J. Appl. Phys.*, vol. 56, no. 7S1, 2017, Art. no. 07JC07.
- [25] R. Kaune, "Accuracy studies for TDOA and TOA localization," in *Proc. 15th Int. Conf. Inf. Fusion (FUSION)*, Jul. 2012, pp. 408–415.
- [26] Z. Jiang, W. Xi, X.-Y. Li, J. Zhao, and J. Han, "HiLoc: A TDoA-fingerprint hybrid indoor localization system," Microsoft Indoor Localization Competition, Tech. Rep., 2014, p. 600.
- [27] B. Xu, R. Yu, G. Sun, and Z. Yang, "Whistle: Synchronization-free TDOA for localization," in *Proc. Int. Conf. Distrib. Comput. Syst.*, Jun. 2011, pp. 760–769.
- [28] J. Xu, M. Ma, and C. L. Law, "Cooperative angle-of-arrival position localization," *Measurement*, vol. 59, pp. 302–313, Jan. 2015.

- [29] S. Ogiso, T. Kawagishi, K. Mizutani, N. Wakatsuki, and K. Zempo, "Self-localization method for mobile robot using acoustic beacons," *ROBOMECH J.*, vol. 2, no. 1, 2015, Art. no. 12.
- [30] H. Iwaya, S. Ogiso, K. Mizutani, T. Ebihara, and N. Wakatsuki, "Effect of movement on positioning accuracy in a transponder-based acoustical positioning," *J. Phys., Conf. Ser.*, vol. 1075, no. 1, 2018, Art. no. 012025.
- [31] S. Ogiso, K. Mizutani, N. Wakatsuki, and T. Ebihara, "Evaluation of time-difference-of-arrival error of acoustic beacons caused by velocity of microphone array," *J. Phys., Conf. Ser.*, vol. 1075, no. 1, 2018, Art. no. 012046.
- [32] H. Liu, H. Darabi, P. Banerjee, and J. Liu, "Survey of wireless indoor positioning techniques and systems," *IEEE Trans. Syst., Man, Cybern. C, Appl. Rev.*, vol. 37, no. 6, pp. 1067–1080, Nov. 2007.
- [33] A. H. Moore, C. Evers, and P. A. Naylor, "Direction of arrival estimation in the spherical harmonic domain using subspace pseudointensity vectors," *IEEE/ACM Trans. Audio, Speech, Lang. Process.*, vol. 25, no. 1, pp. 178–192, Jan. 2017.
- [34] R. Tanabe, Y. Sasaki, and H. Takemura, "Probabilistic 3D sound source mapping system based on Monte Carlo localization using microphone array and LiDAR," *J. Robot. Mechatron.*, vol. 29, no. 1, pp. 94–104, 2017.
- [35] S. Ogiso, K. Mizutani, N. Wakatsuki, and T. Ebihara, "Robust localization of mobile robot in reverberant rooms using acoustic beacons with iterative Bayesian filtering," in *Proc. 9th Int. Conf. Indoor Positioning Indoor Navigat.*, Sep. 2018, pp. 1–6.
- [36] J. R. Klauder, A. C. Price, S. Darlington, and W. J. Albersheim, "The theory and design of chirp radars," *Bell Syst. Tech. J.*, vol. 39, no. 4, pp. 745–808, Jul. 1960.



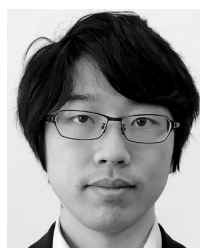
KOICHI MIZUTANI was graduated from National Defense Academy, in 1979, and the Ph.D. degree in engineering from Kyoto University, in 1990. He was a Researcher with the Department of Electrical Engineering, National Defense Academy, from 1984 to 1988, and with the Department of Research of the Communication and Intelligence, School of Japanese Ground Self Defense Force (JGSDF), from 1988 to 1990. He was the Deputy Director of the Secretariat of Director General of the National Defense Agency, from 1991 to 1992. He retired from the JGSDF at the rank of Major. He joined as an Assistant Professor with the Faculty of the Institute of Applied Physics, University of Tsukuba, in 1992, where he is currently a Professor with the Faculty of Engineering, Information and Systems. He has been engaged in researches on medical electronics, welfare technologies, complement of human sensory functions, robot sensing, communication system in sensing grid, environment monitoring, applied optics, applied acoustics, musical acoustics, food and agricultural engineering, and health monitoring engineering of livestock. He is a member of the IEICE, the Institute of Electrical Engineering (IEE) of Japan, The Japan Society of Mechanical Engineering (JSME), The Society of Agricultural Structures, Japan (SASJ), the Virtual Reality Society of Japan (VRSJ), the Marine Acoustics Society of Japan (MASJ), The Japanese Society for Food Science and Technology, the Japan Society of Civil Engineering (JSCE), the Japan Society of Applied Physics (JSAP), and the Architectural Institute of Japan (AIJ).



NAOTO WAKATSUKI received the B.Eng., M.Eng., and D.Eng. degrees from the University of Tsukuba, in 1993, 1995, and 2004, respectively. He was with Okayama University, from 1995 to 2001, and Akita Prefectural University, from 2001 to 2006. He is currently an Associate Professor with the University of Tsukuba. His research interests include acoustic instrumentation, simulation-based visualization, vibration sensors and actuators, acoustical engineering, musical acoustics, and inverse problems. His affiliated academic societies include the Acoustical Society of Japan, Acoustical Society of America, The society of Agricultural Structures, and Japan Society for Simulation Technology.



TADASHI EBIHARA was born in Tokyo, Japan, in 1986. He received the Ph.D. degree from the University of Tsukuba, Tsukuba, Japan, in 2010. From September 2013 to December 2013, he was a Visiting Professor with the Delft University of Technology, The Netherlands. He is currently an Associate Professor with the Faculty of Engineering, Information and Systems, University of Tsukuba. His research interests include mobile communications and their applications to underwater acoustic communication systems. He received the Research Fellowship for Young Scientists (DC1) from the Japan Society for the Promotion of Science (JSPS), for the years 2009 and 2010. He received the 2017 IEEE Oceanic Engineering Society Japan Chapter Young Researcher Award.



SATOKI OGISO was born in Gifu, Japan, in 1991. He received the Ph.D. degree from the University of Tsukuba, Tsukuba, Japan, in 2019. He is currently an Assistant Professor with the Department of Electronic Control Systems, National Institute of Technology, Gifu College. His research interests include acoustical signal processing, acoustical indoor positioning, and bone-conducted sound assessment. He received the Research Fellowship for Young Scientists (DC1) from the Japan Society for the Promotion of Science (JSPS), for the years 2016–2018. His affiliated academic societies include the IEEE, Acoustical Society of Japan, Acoustical Society of America, Japan Society of Civil Engineers, and The Japan Society of Mechanical Engineers.

...